Release of natural extracts from PVA and PVA-CMC hydrogel wound dressings: a power law swelling/delivery

Renata Nunes Oliveira[1]*, Luiz Augusto da Cruz Meleiro[1], Brid Quilty[2] and Garrett Brian McGuinness[3]

[1]Chemical Engineering Department, Institute of Technology, Federal Rural University of Rio de Janeiro, Rio de Janeiro, Brazil, [2]School of Biotechnology, Dublin City University, Dublin, Ireland, [3]School of Mechanical and Manufacturing Engineering, Dublin City University, Dublin, Ireland

Introduction: PVA hydrogels present many characteristics of the ideal dressing, although without antimicrobial properties. The present work aims to study the physical, mechanical and release characteristics of hydrogel wound dressings loaded with either of two natural herbal products, sage extract and dragon's blood.

Methods: Fourier Transform Infrared Spectroscopy (FTIR), Differential Scanning Calorimetry (DSC) and tensile mechanical testing were used to investigate the structure and properties of the gels. Swelling and degradation tests were conducted according to ISO 10993-9. Release characteristics were studied using UV Spectrophotometry.

Results: PVA matrices incorporating sage extract or dragon's blood (DB) present hydrogen bonding between these components. PVA-CMC hydrogels containing sage present similar spectra to PVA-CMC alone, probably indicating low miscibility or interaction between the matrix and sage. The opposite is found for DB, which exhibits more pronounced interference with crystallinity than sage. DB and NaCMC negatively affect Young's modulus and failure strength. All samples appear to reach equilibrium swelling degree (ESD) in 24 h. The addition of DB and sage to PVA increases the gels' swelling capacity, indicating that the substances likely separate PVA chains. The inclusion of CMC contributes to high media uptake. The kinetics profile of media uptake for 4 days is described by a power-law model, which is correlated to the drug delivery mechanism.

Discussion: A PVA-CMC gel incorporating 15% DB, the highest amount tested, shows the most favorable characteristics for flavonoid delivery, as well as flexibility and swelling capacity.

KEYWORDS

Dragon's blood, sage extract, PVA, hydrogel, wound dressing

1 Introduction

Skin is a vast complex organ, responsible for protecting the body, as well as for regulation of homeostasis. The epidermis is the external layer of skin, which prevents the penetration of stressors, while the dermis is the second (internal) layer containing fat and is responsible for the elasticity of the skin (Cua et al., 1990). Older skin has limited repair capacity and a slow wound healing rate, which in turn facilitates the development of chronic wounds, especially if

the patient already has a chronic condition (Takahashi et al., 2004; Xiao et al., 2022). Dry skin and itching may result in a wound, which allied to low vascularization and innervation, may delay healing (Bánvölgyi et al., 2022). A hydrogel is a hydrophilic polymeric gel layer, physical or chemically crosslinked, presenting structural integrity when hydrated. Hydrogels are typically non-adherent to the wound site, relieve pain, stimulate autolytic *debridement* and present several characteristics associated with ideal dressings (Brumberg et al., 2021).

Hydrogels that are biocompatible and absorb wound exudate while swelling in biological fluids stimulate the healing process, especially biodegradable hydrogels containing reactive oxygen species (Yu et al., 2022). Among hydrogels, *in-situ* chemically crosslinked hydrogels can bind effectively to living tissue, protecting wounds from exterior damage, as well as replicating the barrier properties, vapor transmission and other functions of skin) (Yang et al., 2016). On the other hand, physically crosslinked hydrogels are also interesting for wound healing and can be manufactured to reach properties that mimic skin. Double-network hydrogels have promise for wearable biosensors (monitoring biological fluids), drug delivery systems and scaffolds (Guo et al., 2023).

Traditional hydrogels protect the wound site from secondary infection by preventing permeation of microorganisms toward the wound. However, to treat infected wounds, antibacterial hydrogels are recommended. These gels kill bacteria and allow oxygen transport which stimulates healing (Liu et al., 2022). Infection is a main risk factor for elderly people suffering with wounds (Mattera et al., 2014). Many senior people live in long-term care facilities, places in which infection by methicillin resistant *Staphylococcus aureus* (MRSA) is potentially found (Augustine and Bonomo, 2011). Natural products such as honey have been used as a wound covering material, presenting faster and complete healing with low odour (Zeleníková and Vyhlídalová, 2019). In another example, infection caused by antibiotic resistant *S. aureus* and *Pseudomonas aeruginosa* (bacteria that colonize wounds) have been successfully treated by the synergistic effect of *Rumex abyssinicus* and *Discopodium penninervium* in a blend of essential oils (Gadisa and Usman, 2021). MRSA infection has also been successfully treated *in-vitro* by *Cinnamomum impressicostatum* stem-bark water extract (Buru et al., 2014).

Salvia officinalis (sage) hydroalcoholic extracts have been shown to present anti-inflammatory and antioxidant activities. Sage has been shown to regulate the expression of pro-inflammatory cytokines, growth factors, and antioxidant properties, stimulating wound healing (Farahpour et al., 2020). Wounds treated with 5% Sage extract presented high re-epithelialization, wound contraction and angiogenesis (Karimzadeh and Farahpour, 2017). In addition, *S. officinalis* essential oil (which contains cis-thujone, camphor, trans-thujone and 1,8-cineole) was incorporated into gelatin hydrogels and their *S. aureus* and *E. coli* inhibition halos were similar to silver nanoparticles ones (Gherman et al., 2018). Dragon's blood is a reddish resin extracted directly from the *Croton lechleri* tree (exudated by the tree stem when it is cut) (Peres et al., 2023). *Croton Lechleri* (Dragon's blood) is a resinous material with anti-inflammatory, antioxidant and healing properties, probably attributable to phenolic compounds and alkaloid taspine (Gupta et al., 2008; Namjoyan et al., 2016). In Dragon's blood, gallic acid, syringic acid, epicatechin and catechin are the most prevalent active substances (Diedrich et al., 2021). Dressings of oxidized hyaluronic acid

and carboxymethyl chitosan loaded with Dragon's blood from China showed sustained release of Loureirin A and Loureirin B (active compounds), accelerating healing of burns *in-vivo* (Xu et al., 2022).

Among the many hydrogels available for the incorporation of natural antibacterial products, common choices are polyvinyl alcohol (PVA) and sodium carboxymethyl cellulose (denoted 'CMC' in this work). PVA is a non-toxic, hydrophilic, biocompatible material while CMC is highly hydrophilic and a low-cost material. PVA and CMC can be mixed to adjust the resultant hydrogels' functional properties (Djumaev and Tashmukhamedova, 2020). As an example of the usage of these gels as delivery systems, the release and erosion characteristics of PVA-CMC hydrogels laden with Inebrin have been successfully studied (Djumaev and Tashmukhamedova, 2020), as well as the release effect of PVA-CMC gels incorporating Cu nanoparticles and their positive activity against *S. aureus* and *E. coli* (Ponco and Helmiyati, 2020). As part of a broader study to evaluate natural products selected based on published evidence of their use as topical wound treatments, Sage extract and dragon's blood, along with Propolis from two sources and Pomegranate, were previously characterized for their composition and antioxidant activity (Oliveira et al., 2016). Dragon's blood exhibited amongst the highest anti-oxidant activity, but the dragon's blood resin and Sage extract were both found to be in the lower range for phenol and flavonoid content. This means that the physical, chemical, swelling and release characteristics of the proposed PVA and PVA-CMC hydrogels are likely to be of critical importance to their overall efficacy in wound healing. The contribution of a detailed study of PVA-based gels incorporating dragon's blood in particular provides insight into a system on which little information has previously been available.

2 Materials and methods

PVA and PVA-CMC samples were prepared through the dissolution of 10% w/v polymers (from 8 to 10 g of Poly (vinyl alcohol) - PVA, Mw 85.000–124.000 and degree of hydrolysis 99+%, Sigma-Aldrich®, and from 2 to 0 g of sodium carboxymethyl cellulose—NaCMC, 250000 Da, Sigma-Aldrich®), using distilled water (from 100 to 85 mL) and herbals (from 15 to 0 mL), Table 1. The natural products used were Sage Tincture (Fushi Wellbeing, 25%), labelled as "S"; and dragons' blood, (Amazon Therapeutics Laboratories, 100%), named "DB". These have been characterised in a previous publication via FTIR in terms of their chemical bond composition, and presence of phenols and flavonoids (Oliveira et al., 2016). The polymers (total of 10%, Table 1) were dissolved in distilled water at 90°C under mechanical stirring. After dissolution, the solution was kept under stirring until room temperature was reached. Then, the herbals were added under stirring. The amount of DB or S in each sample was based on the amount of each herbal added to the polymers, rather than a post-preparation measurement. 20 mL of each solution was poured on Petri dishes (φ 150 mm), freeze-thawed overnight (at −16°C), and dried in room conditions.

2.1 Physical properties

The Fourier-Transform Infrared Spectroscopy (FTIR) analysis of the samples was performed. The equipment used was Perkin

TABLE 1 2^3 Factorial design with three factors: "Polymer", "Type of drug" and "Amount of drug". Each factor consisted of 2 levels, respectively: PVA and PVA-CMC; Dragon's blood and Sage extract; and from 0 mL to 15 mL of each herbal.

RunOrder	CenterPt	Polymer	Natural product	Amount of drug (mL)	Sample name
1	0	PVA	Dragon's blood	7,5	PVA-7.5DB
2	1	PVA	Sage	15	PVA-15S
3	1	PVA-CMC	Sage	0	PVACMC
4	0	PVA-CMC	Sage	7,5	PVACMC-7.5S
5	0	PVA	Sage	7,5	PVA-7.5S
6	1	PVA-CMC	Dragon's blood	15	PVACMC-15DB
7	0	PVA-CMC	Dragon's blood	7,5	PVACMC-7.5DB
8	1	PVA	Dragon's blood	0	PVA

Elmer Spectrum GX (DCU), 16 scans per samples in the region of $(4,000-650)$ cm^{-1}.

The samples were analysed via differential scanning calorimetry (DSC), equipment Perkin Elmer, DSC 8000 (DCU). 10 mg of each sample was submitted to heating rate of 10°C/min from room temperature to 250°C. To overcome the thermal history of the samples, the second heating cycle was used to obtain the gels' properties: glass temperature (Tg) and melting temperature (Tm). The degree of crystallinity (Xc) was calculated according to Eq. (1). (Yang et al., 2018; Zhu et al., 2020).

$$\chi_c\,(\%) = 100\left(\frac{\Delta H}{w\,(\Delta H_0)}\right) = 100\left(\frac{\Delta H}{138.6w}\right) \qquad (1)$$

w is the weight fraction of PVA; ΔH = sample's heat of melting; ΔH_0 = heat of melting of a pure crystalline PVA sample (138.6 J/g) (Jiang et al., 2014; Oliveira et al., 2019).

At least 6 samples of each composition were cut in dog-bone shape from the swollen hydrogels. After 1 day of swelling in PBS, the samples were submitted to tensile tests at room temperature, (Zwick Z005 Tensile Test Machine), with sandpaper in contact with the sample surface. The tests were performed using a 500 N load cell at a crosshead rate of 10 mm/min until failure. The results of at least 6 samples were evaluated, excluding the samples that presented the lowest and the highest curves. The ultimate tensile strength values (σ) and the Secant modulus values (E) were calculated.

Further characterization was based on the results of at least triplicates. *In-vivo* analysis could elicit further impacts in a living system but is beyond the scope of the present study.

2.2 Swelling and release results

Fluid absorption studies were performed using Phosphate Buffered Saline - PBS, Sigma Aldrich (0.01 M phosphate buffer, 0.0027 M KCl, 0.137 M NaCl), which mimics the inorganic phase of body fluids. The swelling/degradation tests followed the standard ISO 10993-9, where samples of approximately 5 cm^2, weight normalized, were placed in 5 mL of each media. The samples remained in the media at 37°C for 4 days, being weighed at regular time intervals (1 h, 2 h, 4 h, 1 day, and 4 days) to calculate the samples' Swelling Degree (SD) using Eq. (2). After

4 days, the samples were dried and weighed to calculate the gel fraction (GF) and weight loss (WL) using Eqs 3, 4. In these equations, SD_D is the dried samples weight before the swelling tests, SD_{D2} is the dried samples weight after the test, and SD_S is the swollen samples weight.

$$SD\,(\%) = 100\left(\frac{SD_S - SD_D}{SD_D}\right) \qquad (2)$$

$$GF\,(\%) = 100\left(\frac{SD_{D2}}{SD_D}\right) \qquad (3)$$

$$WL\,(\%) = 100\left(\frac{SD_D - SD_{D2}}{SD_D}\right) \qquad (4)$$

The kinetics of drug delivery from hydrogels has been extensively studied. Since delivery can occur simultaneously to the swelling, modelling the swelling degree of samples may indirectly describe the gels' drug delivery. (Setapa et al., 2020). The SD of the samples was modelled by the Korsmeyer-Peppas (Power law) model (Eq. (5)), where $\frac{M_t}{M_\infty}$ is the fraction of drug released, k is the kinetic constant, t is the release time and n is the diffusional exponent of drug release. (Shabbir et al., 2018).

$$\frac{M_t}{M_\infty} = kt^n \qquad (5)$$

The concentration of flavonoids delivered by the gels was measured. 0.5 mL of the swelling media after 4 days (1 mg/mL) was mixed with 0.5 mL of 2% AlCl$_3$ (Sigma-Aldrich) ethanolic solution in the dark (triplicates). To plot a standard curve, 0.5 mL of different solutions of quercetin (Sigma-Aldrich, range of 0 μg–125.00 μg) in ethanol was mixed with 0.5 mL of 2% AlCl$_3$ ethanolic solution in the dark. After incubation for 45 min, the solutions were analysed in the UV-Vis spectrophotometer (VWR, UV-3100PC Spectrophotometer, DCU), wavelength of 415 nm (Oliveira R.N. et al., 2016).

2.3 Statistical analysis

All data that was measured at least in triplicate (maximum of 6 samples) was statistically evaluated. Data with replicas were evaluated in OriginPro 8® by 1-way ANOVA-analysis and Tukey
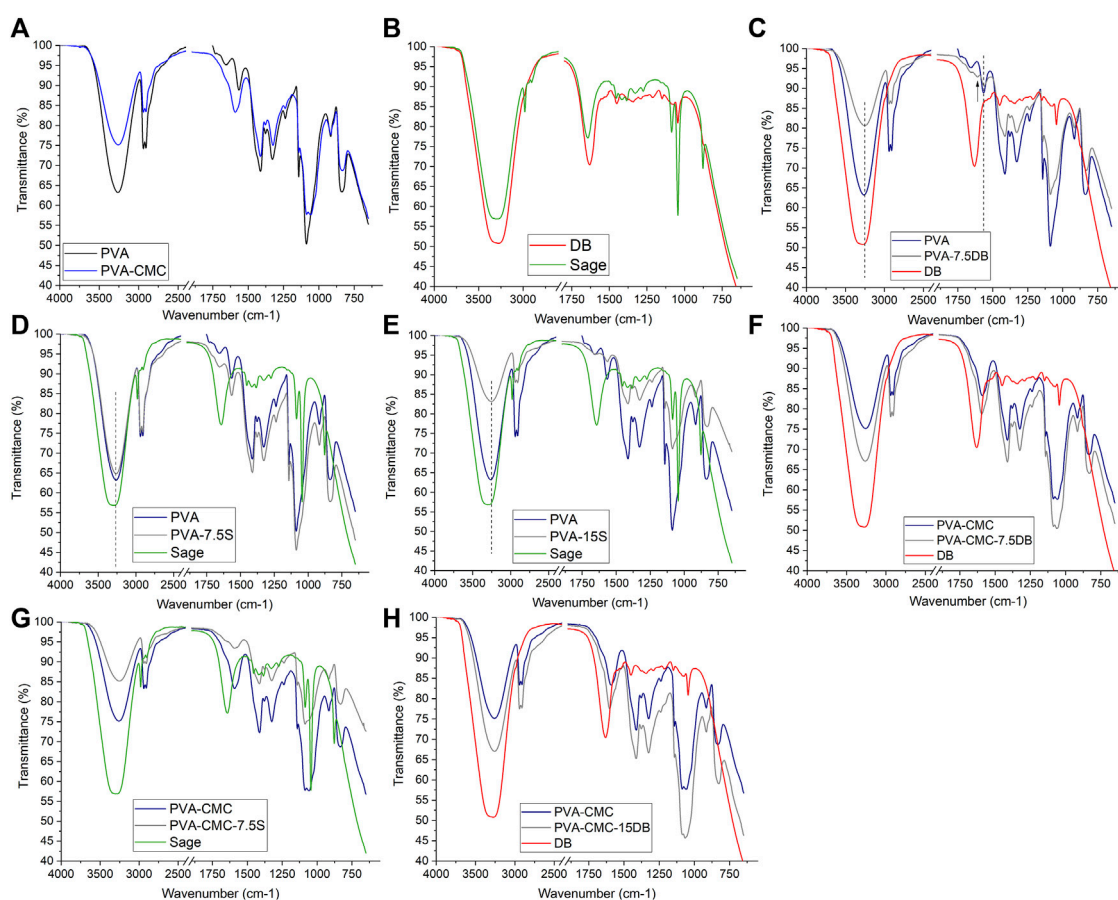
FIGURE 1
FTIR spectra of **(A)** the matrices, PVA and PVA-NaCMC; **(B)** the herbal extracts: sage, and dragon's blood. FTIR spectra of the individual matrix and herbal, as well as the loaded samples: **(C)** PVA-7.5% DB sample; **(D)** PVA-7.5%S; **(E)** PVA-15%S; **(F)** PVA-CMC-7.5% DB; **(G)** PVA-CMC-15% DB; **(H)** PVA-CMC-7.5% S.

test, where the factor was "composition", with 8 levels (the compositions listed in Table 1), value of significance: 95%. All data was used as 'response' in the factorial design, but only the data showing significance in the pareto plot were included in the present work.

3 Results and discussion

3.1 Physical properties

3.1.1 Fourier-transform infrared spectroscopy—FTIR

The polymeric matrices presented the characteristic bands of PVA and Na-CMC, Figure 1A and Table 2. Sage extract and dragon's blood bands, Figure 1B and Table 1, revealed, besides the extracts/plants characteristic bands, an intense band at ~3,300 cm^{-1}, indicative of hydroxyl groups contribution of ethanol, since they are herbal extracts (Jadhav et al., 2017). In both spectra there is a band at approximately 1,080 cm^{-1}, related to ethanol's $\delta(C - O - C)$ vibration (Pangesti and Masruri, 2020).

All samples presented the characteristic FTIR bands of the matrix and of the herbals. The differences encountered are highlighted as follows, firstly the PVA matrix samples and then, PVA-matrix samples. The PVA matrices loaded with the herbals (sage or DB), Figure 1, presented displacement of the PVA bands at 3,270 cm^{-1} ($v(-OH)$) (Choo et al., 2016; Dmitrenko et al., 2022; Siddaiah et al., 2018) and at 840 cm^{-1} ($v(C - C)$) (Choo et al., 2016; Dmitrenko et al., 2022) toward lower wavenumbers (indicated by dash lines in Figures 1C–E). Since these bands at lower wavenumber were not identified in the isolated materials (PVA, sage or dragon's blood), they might be related to physical interactions between components. Since both herbals and matrices present -OH groups, hydrogen bonding may have occurred (Fathi et al., 2011). The $v(C - C)$ displacement could be attributed to Wan der Waals interactions between the matrix and the herbal extract. PVA-7.5DB sample presented displacement of a band from 1,567 cm^{-1} ($v(C = C)$) (Choo et al., 2016; Siddaiah et al., 2018) to 1,560 cm^{-1}, as well as the presence of a band at 1,608 cm^{-1} (indicated by an arrow in Figure 1C), besides all bands of PVA and DB. This could be related to oxidative process (Abdel Bary et al., 2018), as well as to specific chemical interaction between PVA and DB (Akhlaq et al., 2021).

The PVA-CMC-7.5DB and PVA-CMC-15DB (named in Table 1) presented patterns similar to PVA-CMC. The slight

TABLE 2 FTIR bands of the matrixes (PVA and PVA-CMC) and of the herbal extracts (dragon's blood and sage).

Wavenumber (cm^{-1})	Vibration mode	References
PVA		
3,270	$\upsilon(-OH)$ of free alcohols	Choo et al. (2016); Dmitrenko et al. (2022); Siddaiah et al. (2018)
2,941	Alkyl's $\upsilon(C-H)$	Reis et al. (2006), Mohamed et al. (2022)
2,908	$\upsilon(CH_2)$	Dmitrenko et al. (2022)
1,655; 1,567	$\upsilon(C=C)$	Choo et al. (2016), Siddaiah et al. (2018)
1,413	$\delta_s(CH_2)$; $\delta(O-H)$	Dmitrenko et al. (2022); Salazar (2018)
1,378	$\delta(C-H)$; $\delta(O-H)$	Salazar (2018)
1,328	CH; $\delta(OH)$	Reis et al. (2006); Mohamed et al. (2022)
1,237	$(C-H)$	Zhang et al. (2020)
1,143	$\upsilon(C-O)$; $\upsilon(C-C)$; $crystallinity$	Reis et al. (2006), Salazar (2018)
1,088	$\upsilon(C-O)$	Choo et al. (2016); Salazar (2018); Siddaiah et al. (2018); Mohamed et al. (2022)
916	$\rho(CH_2)$; $\upsilon(C-C)$	Dmitrenko et al. (2022); Salazar (2018); Siddaiah et al. (2018)
840	$\upsilon(C-C)$ of planar zigzag carbon backbone	Choo et al. (2016); Dmitrenko et al. (2022)
PVA-CMC		
3,260	$\upsilon(-OH)$	Choo et al., 2016; Dmitrenko et al. (2022); Siddaiah et al. (2018); Sharratt et al. (2021)
2,940	PVA's Alkyl's $\upsilon(C-H)$; NaCMC's aliphatic $\upsilon(C-H)$	Reis et al. (2006); Kadry (2019); Mohamed et al. (2022)
2,908	PVA's $\upsilon(CH_2)$; NaCMC's $\upsilon(C-H)$	Dmitrenko et al. (2022); Devi et al. (2020)
1,591	NaCMC's $\upsilon_{as}(COO^-)$	Pettignano et al. (2019)
1,412	PVA's $\delta_s(CH_2)$; $\delta(O-H)$; NaCMC's $\upsilon_{as}(COO^-)$	Dmitrenko et al. (2022), Salazar (2018); Kadry (2019)
1,378	PVA's $\delta(C-H)$; $\delta(O-H)$	Salazar (2018)
1,325	$\delta(OH)$	Reis et al. (2006); Devi et al. (2020); Mohamed et al. (2022)
1,238	PVA's $(C-H)$	Zhang et al. (2020)
1,142	PVA's $\upsilon(C-O)$; $\upsilon(C-C)$; $crystallinity$	Reis et al., 2006; Salazar, 2018
1,086	PVA's $\upsilon(C-O)$; $NaCMC's \upsilon(C-O-C)$	Choo et al. (2016); Salazar (2018); Siddaiah et al. (2018); Kadry (2019); Mohamed et al. (2019)
1,060	NaCMC's $\upsilon(-C-O)$ of polysaccharide skeleton	Devi et al. (2020)
916	PVA's $\rho(CH_2)$; $\upsilon(C-C)$	Dmitrenko et al. (2022); Salazar (2018); Siddaiah et al. (2018)
834	PVA's $\upsilon(C-C)$ of planar zigzag carbon backbone	Choo et al. (2016); Dmitrenko et al. (2022)
Dragon's Blood resin (DB)		
3,295	$\upsilon(-OH)$	Jadhav et al. (2017)
1,631	$\upsilon(C=C)$ of aromatics	Koperska et al. (2011); Silva and Rodriguez (2019)
1,451	Angular deformation of $(C-O)$ bond in $COOH$; $\upsilon(C=C)$ of aromatics	Koperska et al. (2011); Silva and Rodriguez (2019)
1,340	$(C-C)$	Koperska et al. (2011)
1,297	Angular deformation of $(C-O)$ bond in alcohols and phenols	Silva and Rodriguez (2019)
1,214	$(C-O)$ of $COOH$; $\upsilon(O-CH_3)$; Angular deformation of (C-O) bond in alcohols and phenols	Koperska et al. (2011); Salguero and Pilaquinga (2011)

TABLE 2 (*Continued*) FTIR bands of the matrixes (PVA and PVA-CMC) and of the herbal extracts (dragon's blood and sage).

Wavenumber (cm^{-1})	Vibration mode	References
1,149	Angular deformation of $(C - O)$ bond in alcohols and phenols	Silva and Rodriguez (2019)
1,073		
1,045		
Sage Extract		
3,304	*phenolic* $\upsilon(-OH)$	Salević et al. (2022)
2,980	$\upsilon(C - H)$	Galvin-King et al. (2019)
2,904	*phenolic* $(-OH)$; aliphatic $\upsilon(C-H)$; CH_3, CH_2 (C_{sp}^3, C_{sp}^2)	Mot et al. (2022); Salević et al. (2022)
1,643	*carbonyl group's* $\upsilon(C = O)$; $\upsilon(C = C)$ of $(>C = CH_2)$, $(-CH = CH-)$, $(-CH = C<)$	Mot et al. (2022)
1,454	$(C = C)$, $(C = N)$, $(C = O)$; $\delta_{s,as}(C - H)$ of CH_2 and CH_3 groups; $\delta_{in\ plane}(C - H)$; $\upsilon_{s,as}(C - O)$; $\delta_{in\ plane}(O - H)$; $\delta_s(CH_3, CO)$; $\upsilon_{s,as}(C - O - C)$	Galvin-King et al. (2019); Mot et al. (2022)
1,418	υ, δ (aromatic ring)	Salević et al. (2022)
1,385	$(C = C)$, $(C = N)$, $(C = O)$; $\delta_{s,as}(C - H)$ of CH_2 and CH_3 groups; $\delta_{in\ plane}(C - H)$; $\upsilon_{s,as}(C - O)$; $\delta_{in\ plane}(O - H)$; $\delta_s(CH_3, CO)$; $\upsilon_{s,as}(C - O - C)$	Galvin-King et al. (2019); Mot et al. (2022)
1,328		
1,275	$\delta(C - H)$; $\delta(O - H)$	Salević et al. (2022)
1,086	$\delta_{s,as}(C - H)$ of CH_2 and CH_3 groups; $\delta_{in\ plane}(C - H)$; $\upsilon_{s,as}(C - O)$; $\delta_{in\ plane}(O - H)$; $\delta_s(CH_3, CO)$; $\upsilon_{s,as}(C - O - C)$	Mot et al. (2022)
1,044		
877	$\omega_{out-of-plane}(CH_2, CH)$; $\delta_{out-of-plane}(O - H)$	Mot et al. (2022)

changes were the overlap of the DB bands with the PVA-CMC ones (Figures 1F,G) (Neres Santos et al., 2019). The similarity to the PVA-CMC spectrum probably indicates low miscibility or interaction between the matrix and sage extract (da Silva Cabral and Jose Felix Carvalho, 2019). There was physical interaction between PVA and the herbals, and an oxidative process was identified in PVA-7.5 DB sample. PVA-CMC samples presented mostly PVA-CMC bands and low influence of the herbal bands.

3.1.2 Differential scanning calorimetry – DSC

The polymeric samples loaded with natural products presented higher Tg and lower Tm and Xc compared to the polymeric matrices themselves (PVA and PVA-CMC samples), Figure 2. By adopting Tg, Tm and Xc data as factorial design responses, it was observed that the amount of extract was a significant factor for Xc and Tm, while the type of extract was the determinant parameter for the Tg results, Figures 2C–E. The addition of Dragon's blood resulted in higher Tg than for sage extract. High Tg in the presence of the extracts means that the amorphous polymeric chains need more heat for chains to move. High Tg would be due to hydrogen bonding formation between chains, as the FTIR spectra indicated by changes in the spectra (Campos et al., 2013). Low Tm and Xc represent interference of the herbals with the ability of chains to pack into crystallites, resulting in fewer imperfect crystallites being

formed (Peng et al., 2015). There is a lower transition temperature from amorphous to crystalline (Siddaiah et al., 2018). In addition, the low Xc indicates that DB interferes with contact between PVA chains and that there is compatibility or miscibility between PVA and DB components compared to sage, in agreement with the FTIR results (Restrepo et al., 2018). It is clearly observed that DB interferes with the samples' crystallinity (lowering it) more pronouncedly than sage. The samples containing sage present high crystallinity, where the Tm is slightly shifted to low temperatures, Figures 2F–H. This could be attributed to the effect of the herbals' molecules being positioned between the polymer chains, weakening the connections between them (Campos et al., 2013).

Amorphous and crystalline gels result in different rates of degradation (weight loss - WL) and drug delivery rate. More crystalline gels usually present slow WL and drug delivery, with samples presenting the highest Xc and Tm being the slowest. By that measure, the best composition would be PVA-CMC without any herbal constituent. However, since the goal of this work was to slowly delivery phenols and flavonoids to the wound site, it is observed that PVA-CMC loaded with sage presented the highest Xc and Tm among the studied samples. These gels also present relatively low Tg, indicating facilitation of the movement of chains in the matrix, which would make the membranes more conformable. Samples with low Tg, Tm and Xc would be soft and comfortable to user.
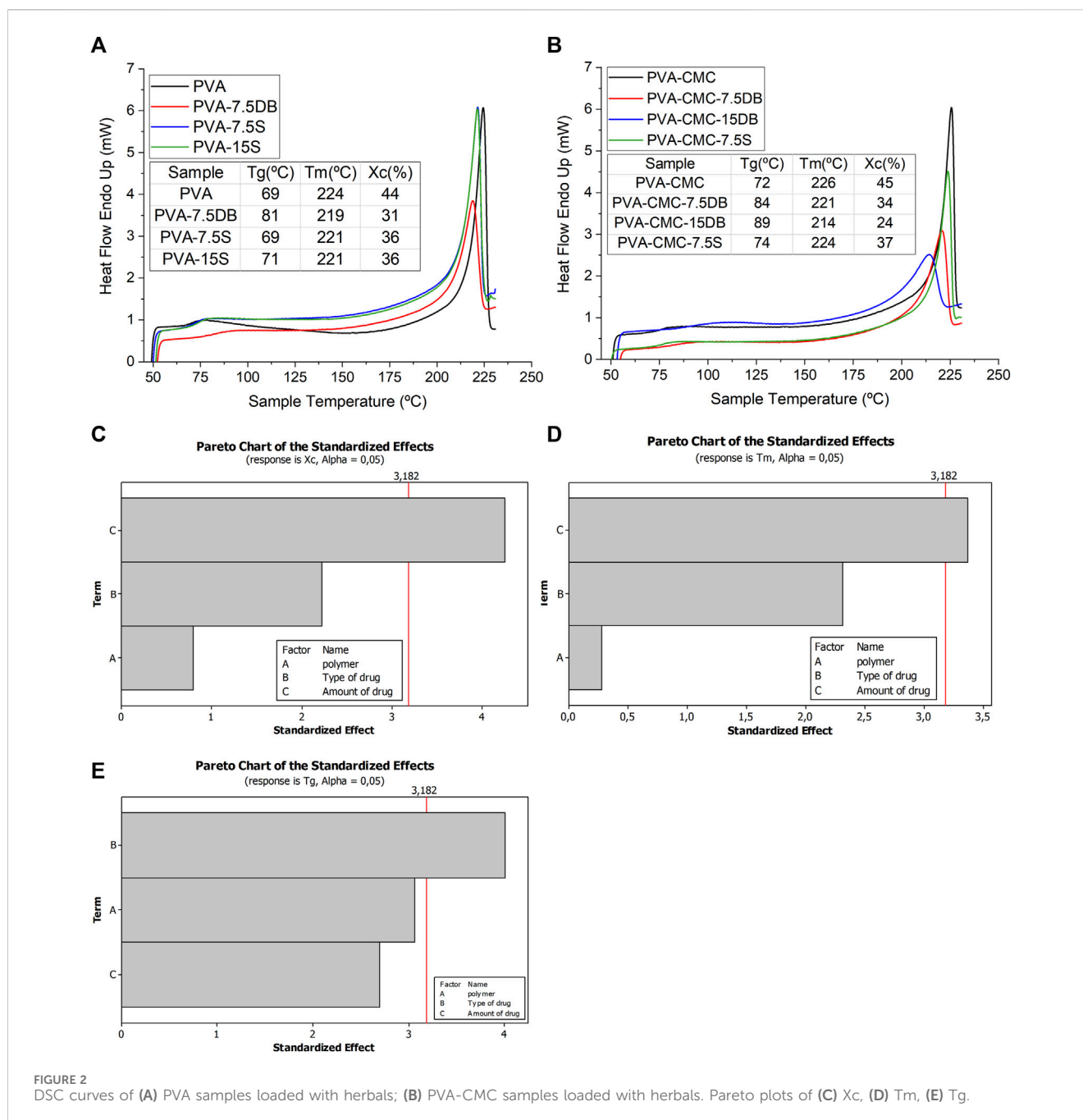
FIGURE 2
DSC curves of **(A)** PVA samples loaded with herbals; **(B)** PVA-CMC samples loaded with herbals. Pareto plots of **(C)** Xc, **(D)** Tm, **(E)** Tg.

3.1.3 Mechanical properties

The mechanical properties of swollen samples were evaluated by ANOVA−1 way analysis (factor "composition", 8 levels) as well as by the MINITAB software regarding the factorial design responses (average results of Young's modulus, "E", and failure strength, "s"), Figure 3. The type of matrix (PVA or PVA-CMC) is the significant parameter for the mechanical properties studied (Figure 3, Pareto plots).

PVA-CMC presents a low Young's modulus and failure strength compared to PVA samples. Since NaCMC mechanical properties are considered poor compared to the PVA ones, this trend was expected (Tarawneh et al., 2021; Cyriac et al., 2022). Sodium carboxymethyl cellulose is obtained through carboxymethylation reaction, where

low weight molecules can be extracted from the cellulose fibres. These oligomers may act as plasticizers ("small" molecules between polymeric chains, separating them), resulting in poor mechanical properties (Siqueira et al., 2015).

DB and NaCMC negatively affect the Young's modulus ($p < 0.05$), which is in line with the Tm and Xc results from DSC. Since Young's modulus is associated with the degree of bonding strength (Zeinalipour-Yazdi and Christofides, 2009), NaCMC is believed to interfere with PVA chain packing. NaCMC also diminishes failure strength ($p < 0.05$). The more extensible gels are, the more comfortable they may be to the patient. In the present work, the stiffness of all gels were similar or higher than 0.02–0.05 MPa, which is the reported skin stiffness of patients older than 30 years-old
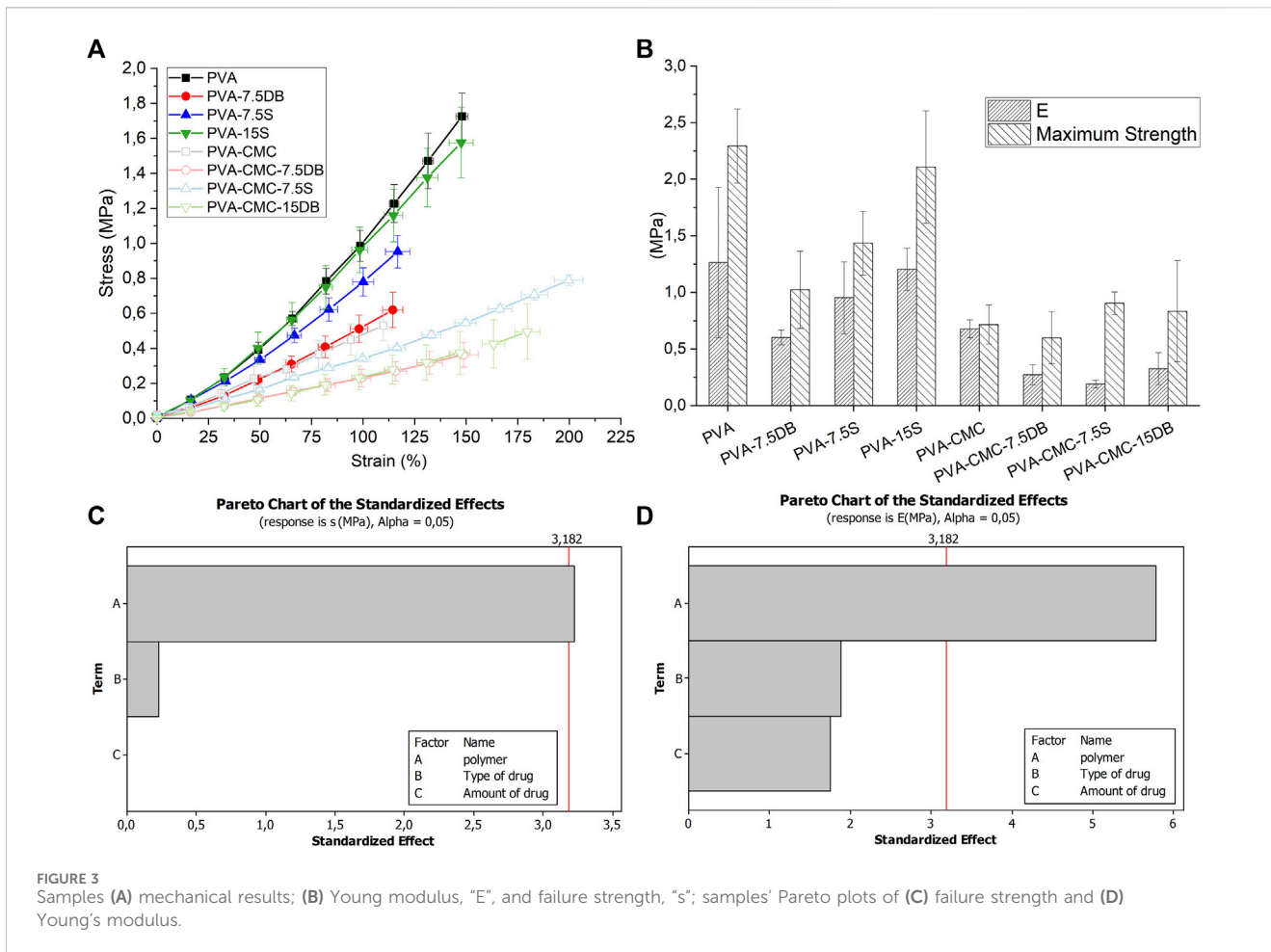
FIGURE 3
Samples **(A)** mechanical results; **(B)** Young modulus, "E", and failure strength, "s"; samples' Pareto plots of **(C)** failure strength and **(D)** Young's modulus.
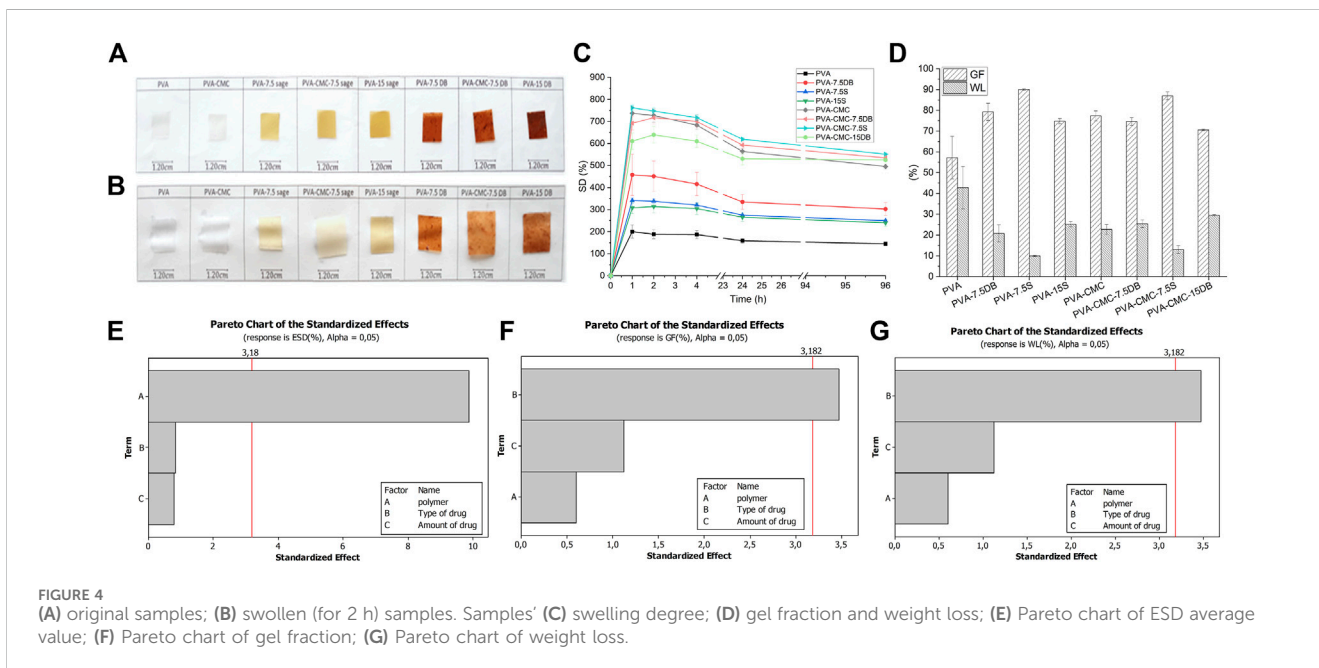

FIGURE 4
(A) original samples; **(B)** swollen (for 2 h) samples. Samples' **(C)** swelling degree; **(D)** gel fraction and weight loss; **(E)** Pareto chart of ESD average value; **(F)** Pareto chart of gel fraction; **(G)** Pareto chart of weight loss.

(Joodaki and Panzer, 2018). The lower stiffness gels were considered the most promising ones, specifically PVA-CMC gels loaded with 15% S or 15% DB.

3.1.4 Swelling and release results

The samples swelling capacities are shown in Figure 4. After 2 h of swelling, the size gain is visible (Figures 4A,B). The samples seemed to
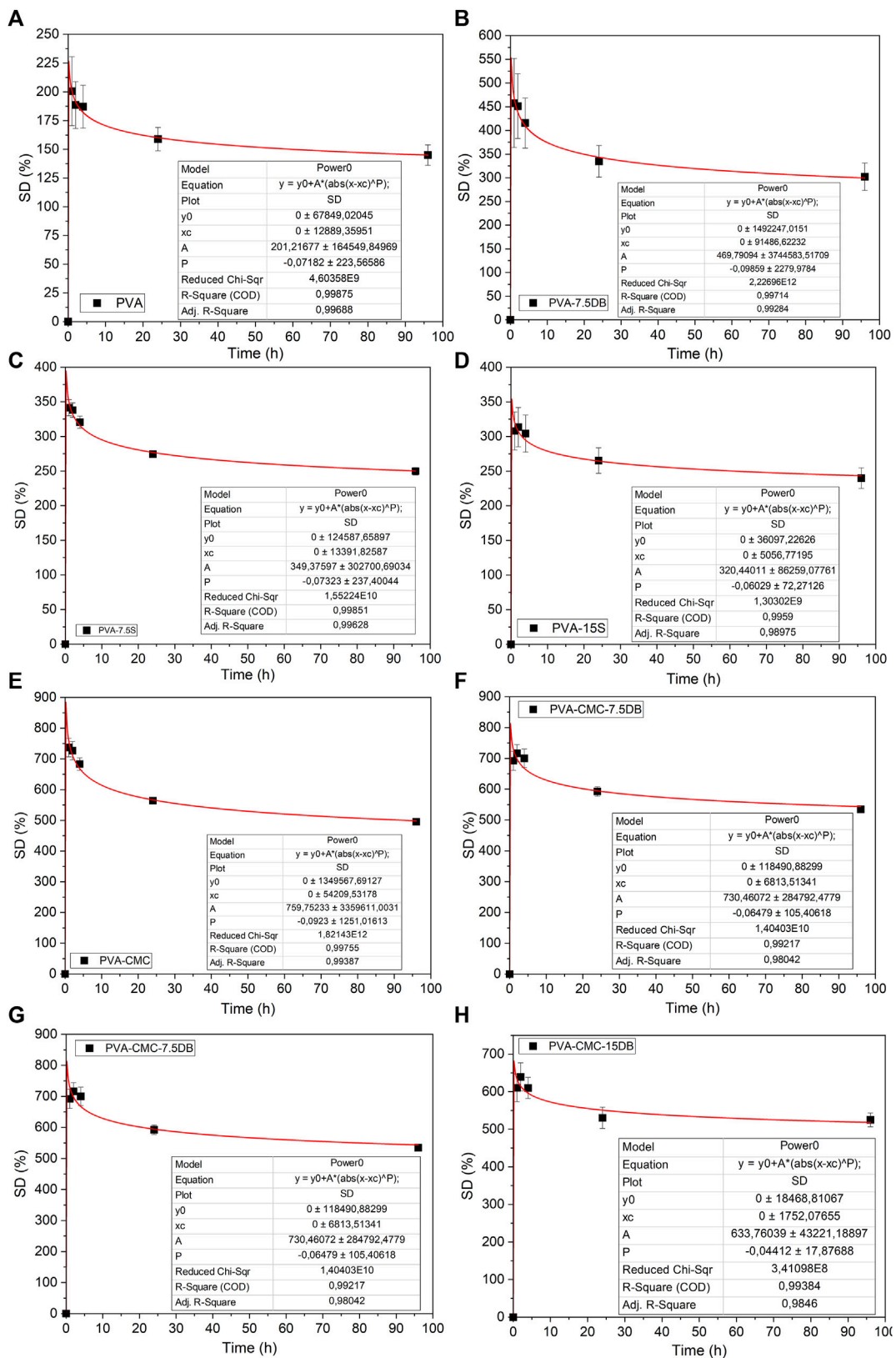
FIGURE 5
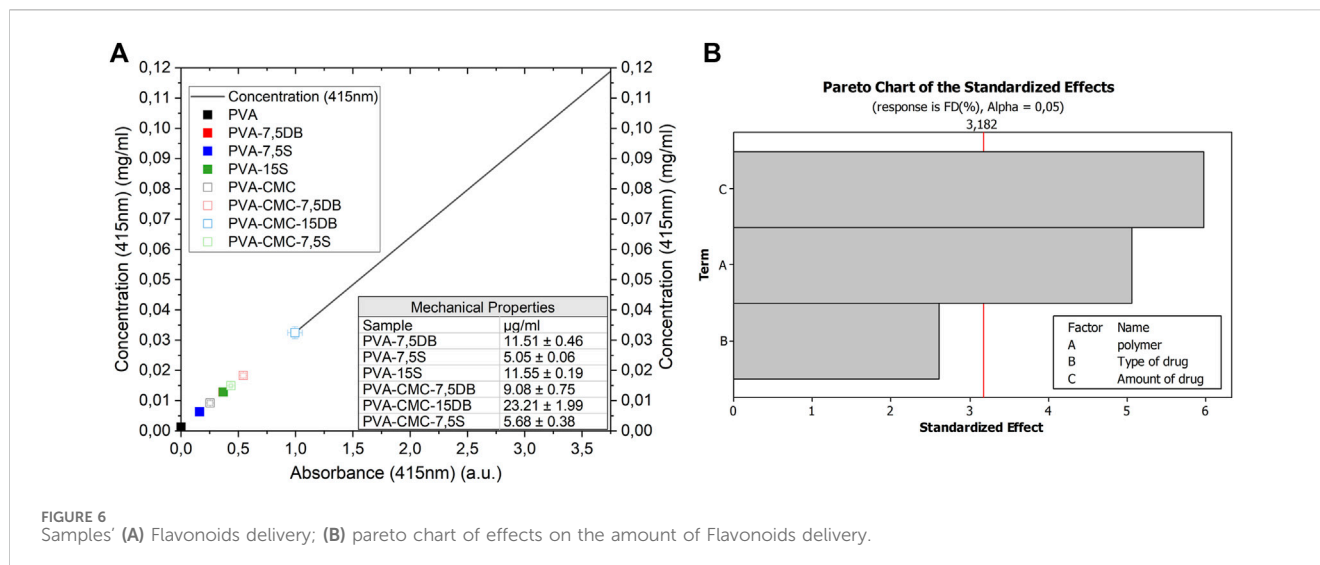Samples **(A–H)** swelling degree modelling by the Power law.

FIGURE 6
Samples' **(A)** Flavonoids delivery; **(B)** pareto chart of effects on the amount of Flavonoids delivery.

reach the equilibrium swelling degree (ESD) in 24 h, Figure 4C. ESD is determined by the equilibrium between the elastic forces of the network and the polymer relaxation (Catoira et al., 2019). The type of matrix (factor "polymer") determines the significant differences between the samples swelling degree (p< 0.05), where samples with CMC present higher swelling capacity, Figure 4 (c, e, h). The high water uptake of gels containing NaCMC is expected, since NaCMC hydrogels are considered superabsorbent, influenced by the high free volume of the network allied with the high hydrophilicity of NaCMC (Basu et al., 2018; Soares et al., 2022). CMC contributes to high media uptake, since it is a highly hydrophilic polysaccharide, diminishing the overall Tm and Xc (Karoyo and Wilson, 2021). Gels/films with high ESD would easily deliver the herbals to the wound site and keep it moisturized (Firlar et al., 2022). In these gels, more water molecules enter the gels' pores and can change places with the herbal substances, thereby delivering them to the wound site. PVA-CMC gels loaded with 15% S or 15% DB could be the ones with the most potential.

Gel fraction and weight loss present opposite trends since they represent the opposite side of the same effect. Weight loss measures the samples' ability to hydrolytically degrade in media (Zhan and Chu, 2002), while gel fraction is an indirect measurement of physical crosslinking (related to effective amorphous entanglements and to PVA crystallites) (Rajawasam et al., 2024). The type of active substance interfered with both gel fraction and weight loss: sage extract resulted in higher gel fraction and lower weight loss compared to dragon's blood, Figure 4. Dragon's blood presented poor water solubility, and if it remained between polymeric chains (Wang et al., 2023), the contact between chains could then be lower, leading to low gel fraction and high weight loss. Although sage extract (hydroalcoholic extract) may also be located between PVA chains, it is a polar extract (Somayeh Samaei et al., 2021), together with water, which facilitates the molecules to exchange places. CMC contributes to high media uptake, since it is a highly hydrophilic polysaccharide, diminishing the overall Tm and Xc (Karoyo and Wilson, 2021). Gels/films with high ESD would easily deliver the herbals to the wound site and keep it moisturized. (Firlar et al., 2022). In these gels, more water molecules enter the gels' pores and can change places with the herbal substances, thereby delivering them to the wound site. PVA-CMC gels

loaded with 15% S or 15% DB could be the ones with the most potential.

The swelling degree was modelled by the Ritger-Peppas equation (Ritger and Peppas, 1987) (p< 0.05), Eq. (5) and Figure 5. Samples' swelling ability was modelled and it is noted that a power-law defines the samples water uptake profile ($R^2 \geq 0.99$). The Peppas equation (Power-law model) is used for drug delivery mechanisms, mainly applied for the first 60% of release, where a Fickian mechanism is proposed (Mircioiu et al., 2019). Although the Peppas model usually describes initial drug release (no more than 60% of release), Korsmeyer-Peppas has also been used to model sustained release (Ge et al., 2022). The Fickian mechanism would be a dose-dependent model, usually occurring below the ESD, when the media penetrates due to the matrix chains mobility and water forces (Ozcan and Didem Saloglu, 2015). When modelling drug release with the Korsmeyer-Peppas equation, the diffusional coefficient "P"<0.5 means that drug release is fast, since it is determined by the water entrance. The interactions between drug and matrix are weak (Frachini et al., 2023), and the hydrogels' swelling follows a Fickian diffusion model (Saidi et al., 2020). Diffusion modelling is usually associated with steric interactions when the hydrogel pores are larger than the active molecules (pores would work as physical reservoirs for the active substance) (Axpe et al., 2019).

3.1.4.1 Flavonoid release

Since PVA and PVA-CMC systems have not previously presented the desired antimicrobial activity (Neres Santos et al., 2019), Dragon's blood and sage extract, containing flavonoids and other active components to control infection, were added. To quantify flavonoid delivery, a standard curve based on quercetin was plotted and the samples' swelling media was evaluated, Figure 6. It can be observed that the PVA-CMC sample interfered with the light transmittance at 415 nm. This is probably due to products of the matrix degradation in the media. To avoid this interference, the values of PVA and PVA-CMC samples were diminished for their respective loaded samples for further analysis. There is a significant difference ($p = 4,49$ E^{-14}) on the concentration of flavonoids delivered, where flavonoid delivery was mainly determined by the type of herbal used, as well as the amount. Since the flavonoids

molecules were much smaller than the gels pore size, their diffusion would be quick. If not, it would indicate that the released substances sizes match the samples' pore size, resulting in slow diffusion (Vigata et al., 2020). As expected, high amounts of herbal in the sample led to a high concentration of flavonoids delivered. Flavonoids are part of the polyphenol substances that usually present limited availability in hydrophilic media due to their lipophilic nature (Costa et al., 2021). Usually, flavonoid activity in wound healing is a synergistic effect of a variety of anti-inflammatory compounds (Carmignan et al., 2020). The addition of DB resulted in almost double the flavonoid delivery compared to sage, and DB is known for accelerating diabetic foot ulcer healing (Rempel et al., 2020). PVA-CMC-15DB would be the preferred sample for flavonoids delivery.

The activity of DB was highlighted in a clinical trial (random, double-blinded study, comprising 60 patients from 14 to 65 years old) when a topic cream loaded with DB significantly diminished the healing times of wounded patients ($p = 0,0001$) (Namjoyan et al., 2016). DB, due to substances present in the dragon's blood, e.g., proanthocyanidins, stimulates wound contraction, formation of new collagen, crust formation and regeneration of the epithelium (Pieters et al., 1995). Regarding Sage, creams with sage extracts led to hydroxyproline production, positively influenced macrophage and fibroblasts distribution, stimulating collagen production and accelerating wound healing (Marques et al., 2023). Characterization of the overall biological response elicited by the hydrogels in the present study, which will be dependent on their composition and relevant to their tissue healing function, is an important future step in this work (Li et al., 2023; Luo et al., 2023).

4 Conclusion

PVA matrices loaded with herbal extracts (sage or DB) presented hydrogen bonding between components. DB interferes with PVA chain contact and there is greater compatibility/miscibility between PVA and DB components compared to sage. It is clearly observed that DB interferes with crystallinity more pronouncedly than sage. DB and NaCMC negatively affect Young's modulus and failure strength. The addition of DB and sage to PVA increased swelling capacity, indicating that the herbal substances remained between PVA chains. PVA-CMC gels loaded with 15% S or 15% DB appear to have better potential regarding high ESD. The kinetics profile of media uptake for 4 days was described by Peppas-Ritger model, which is correlated to the drug delivery mechanism. PVA-CMC-15DB emerged as the most promising system for flavonoid

delivery, ESD, and antioxidant activity. This material should also moisturize the wound site while it releases antimicrobial substances. Further, longer term studies are required to assess the antimicrobial effect in practice, in order to confirm potential to promote the overall healing process.

Data availability statement

The original contributions presented in the study are included in the article/supplementary material, further inquiries can be directed to the corresponding author.

Author contributions

RO: Formal analysis, Funding acquisition, Investigation, Writing–original draft. LM: Formal analysis, Writing–original draft. BQ: Investigation, Writing–original draft. GM: Supervision, Writing–review and editing.

Funding

Conflict of interest

The authors declare that the research was conducted in the absence of any commercial or financial relationships that could be construed as a potential conflict of interest.

Publisher's note

References

Abdel Bary, E. M., Soliman, Y. A., Fekri, A., and Harmal, A. N. (2018). Aging of novel membranes made of PVA and cellulose nanocrystals extracted from Egyptian rice husk manufactured by compression moulding process. *Int. J. Environ. Stud.* 75, 750–762. doi:10.1080/00207233.2018.1456862

Akhlaq, M., Azad, A. K., Ullah, I., Nawaz, A., Safdar, M., Bhattacharya, T., et al. (2021). Methotrexate-loaded gelatin and polyvinyl alcohol (gel/PVA) hydrogel as a pH-sensitive matrix. *Polym. (Basel)* 13, 2300. doi:10.3390/polym13142300

Augustine, S., and Bonomo, R. A. (2011). Taking stock of infections and antibiotic resistance in the elderly and long-term care facilities: a survey of existingand upcoming challenges. *Eur. J. Microbiol. Immunol.* 1, 190–197. doi:10.1556/EuJMI.1.2011.3.2

Axpe, E., Chan, D., Offeddu, G. S., Chang, Y., Merida, D., Hernandez, H. L., et al. (2019). A multiscale model for solute diffusion in hydrogels. *Macromolecules* 52, 6889–6897. doi:10.1021/acs.macromol.9b00753

Bánvölgyi, A., Görög, A., Gadó, K., and Holló, P. (2022). Chronic wounds in the elderly: decubitus, leg ulcers, and ulcers of rare aetiology. *Dev. Heal. Sci.* 4, 81–85. doi:10.1556/2066.2022.00054

Basu, P., Narendrakumar, U., Arunachalam, R., Devi, S., and Manjubala, I. (2018). Characterization and evaluation of carboxymethyl cellulose-based films for healing of full-thickness wounds in normal and diabetic rats. *ACS Omega* 3, 12622–12632. doi:10.1021/acsomega.8b02015

Brumberg, V., Astrelina, T., Malivanova, T., and Samoilov, A. (2021). Modern wound dressings: hydrogel dressings. *Biomedicines* 9, 1235. doi:10.3390/biomedicines9091235

Buru, A. S., Pichika, M. R., Neela, V., and Mohandas, K. (2014). *In vitro* antibacterial effects of Cinnamomum extracts on common bacteria found in wound infections with emphasis on methicillin-resistant *Staphylococcus aureus*. *J. Ethnopharmacol.* 153, 587–595. doi:10.1016/j.jep.2014.02.044

Campos, F., dos, S., Cassimiro, D. L., Crespi, M. S., Almeida, A. E., and Gremião, M. P. D. (2013). Preparation and characterisation of Dextran-70 hydrogel for controlled release of praziquantel. *Braz. J. Pharm. Sci.* 49, 75–83. doi:10.1590/S1984-82502013000100009

Carmignan, F., Matias, R., Carollo, C. A., Dourado, D. M., Fermiano, M. H., Silva, B. A. K., et al. (2020). Efficacy of application of Equisetum pyramidale Goldm. hydrogel for tissue restoration of induced skin lesions in Wistar rats. *Braz. J. Biol.* 80, 12–22. doi:10.1590/1519-6984.184409

Catoira, M. C., Fusaro, L., Di Francesco, D., Ramella, M., and Boccafoschi, F. (2019). Overview of natural hydrogels for regenerative medicine applications. *J. Mater. Sci. Mater. Med.* 30, 115. doi:10.1007/s10856-019-6318-7

Choo, K., Ching, Y., Chuah, C., Julai, S., and Liou, N.-S. (2016). Preparation and characterization of polyvinyl alcohol-chitosan composite films reinforced with cellulose nanofiber. *Mater. (Basel)* 9, 644. doi:10.3390/ma9080644

Costa, R., Costa Lima, S. A., Gameiro, P., and Reis, S. (2021). On the development of a cutaneous flavonoid delivery system: advances and limitations. *Antioxidants* 10, 1376. doi:10.3390/antiox10091376

Cua, A. B., Wilhelm, K.-P., and Maibach, H. I. (1990). Elastic properties of human skin: relation to age, sex, and anatomical region. *Arch. Dermatol Res.* 282, 283–288. doi:10.1007/BF00375720

Cyriac, V., Noor, I. M., Mishra, K., Chavan, C., Bhajantri, R. F., et al. (2022). Ionic conductivity enhancement of PVA: carboxymethyl cellulose poly-blend electrolyte films through the doping of NaI salt. *Cellulose* 29, 3271–3291. doi:10.1007/s10570-022-04483-z

da Silva Cabral, D., and Jose Felix Carvalho, A. (2019). Miscibility of poly(hydroxybutyrate)/poly(vinyl alcohol) melt blends plasticized with glycerol. *J. Renew. Mater.* 7, 325–333. doi:10.32604/jrm.2019.01794

Devi, B. L., Rao, K. M., and Ramananda, D. (2020). Spectroscopic investigation of green synthesized ZnS nanoparticles encapsulated by sodium carboxy methyl cellulose. *Appl. Phys. A* 126, 924. doi:10.1007/s00339-020-04107-y

Diedrich, C., da Silva, L. D., Sari, R., de Cristo Borges, G. C., Muniz, H. S., de Lima, V. A., et al. (2021). Bioactive compounds extraction of Croton lechleri barks from Amazon forest using chemometrics tools. *J. King Saud. Univ. - Sci.* 33, 101416. doi:10.1016/j.jksus.2021.101416

Djumaev, A., and Tashmukhamedova, S. (2020). Physical and chemical properties of polyvinyl alcohol-chemistry manufacturing and controls-based hydrogel carrier loaded with herbal hemostatic agent for application as wound dressings. *Natl. J. Physiol. Pharm. Pharmacol.* 1, 1. doi:10.5455/njppp.2020.10.08214202020082020

Dmitrenko, M., Atta, R., Zolotarev, A., Kuzminova, A., Ermakov, S., and Penkova, A. (2022). Development of novel membranes based on polyvinyl alcohol modified by pluronic f127 for pervaporation dehydration of isopropanol. *Sustainability* 14, 3561. doi:10.3390/su14063561

Farahpour, M. R., Pirkhezr, E., Ashrafian, A., and Sonboli, A. (2020). Accelerated healing by topical administration of Salvia officinalis essential oil on *Pseudomonas aeruginosa* and *Staphylococcus aureus* infected wound model. *Biomed. Pharmacother.* 128, 110120. doi:10.1016/j.biopha.2020.110120

Fathi, E., Atyabi, N., Imani, M., and Alinejad, Z. (2011). Physically crosslinked polyvinyl alcohol–dextran blend xerogels: morphology and thermal behavior. *Carbohydr. Polym.* 84, 145–152. doi:10.1016/j.carbpol.2010.11.018

Firlar, I., Altunbek, M., McCarthy, C., Ramalingam, M., and Camci-Unal, G. (2022). Functional hydrogels for treatment of chronic wounds. *Gels* 8, 127. doi:10.3390/gels8020127

Frachini, E. C. G., Selva, J. S. G., Falcoswki, P. C., Silva, J. B., Cornejo, D. R., Bertotti, M., et al. (2023). Caffeine release from magneto-responsive hydrogels controlled by external magnetic field and calcium ions and its effect on the viability of neuronal cells. *Polym. (Basel)* 15, 1757. doi:10.3390/polym15071757

Gadisa, E., and Usman, H. (2021). Evaluation of antibacterial activity of essential oils and their combination against multidrug-resistant bacteria isolated from skin ulcer. *Int. J. Microbiol.* 2021, 1–8. doi:10.1155/2021/6680668

Galvin-King, P., Haughey, S. A., Montgomery, H., and Elliott, C. T. (2019). The rapid detection of sage adulteration using fourier transform infra-red (FTIR) spectroscopy and chemometrics. *J. AOAC Int.* 102, 354–362. doi:10.5740/jaoacint.18-0341

Ge, M., Li, X., Li, Y., Jahangir Alam, S. M., Gui, Y., Huang, Y., et al. (2022). Preparation of magadiite-sodium alginate drug carrier composite by pickering-emulsion-templated-encapsulation method and its properties of sustained release mechanism by baker–lonsdale and korsmeyer–peppas model. *J. Polym. Environ.* 30, 3890–3900. doi:10.1007/s10924-022-02426-0

Gherman, T., Popescu, V., Carpa, R., Gavril, G. L., Rapa, M., and Oprescu, E. E. (2018). Salvia officinalis essential oil loaded gelatin hydrogel as potential antibacterial wound dressing materials. *REV.CHIM. Buchar.* 69, 410–414. doi:10.37358/RC.18.2.6118

Guo, B., Liang, Y., and Dong, R. (2023). Physical dynamic double-network hydrogels as dressings to facilitate tissue repair. *Nat. Protoc.* 18, 3322–3354. doi:10.1038/s41596-023-00878-9

Gupta, D., Bleakley, B., and Gupta, R. K. (2008). Dragon's blood: botany, chemistry and therapeutic uses. *J. Ethnopharmacol.* 115, 361–380. doi:10.1016/j.jep.2007.10.018

Jadhav, D. L., Karthick, N. K., Kannan, P. P., Shanmugam, R., Elangovan, A., and Arivazhagan, G. (2017). Molecular interaction forces in acetone + ethanol binary liquid solutions: FTIR and theoretical studies. *J. Mol. Struct.* 1130, 497–502. doi:10.1016/j.molstruc.2016.10.055

Jiang, H., Zuo, Y., Zhang, L., Li, J., Zhang, A., Li, Y., et al. (2014). Property-based design: optimization and characterization of polyvinyl alcohol (PVA) hydrogel and PVA-matrix composite for artificial cornea. *J. Mater. Sci. Mater. Med.* 25, 941–952. doi:10.1007/s10856-013-5121-0

Joodaki, H., and Panzer, M. B. (2018). Skin mechanical properties and modeling: a review. *Proc. Inst. Mech. Eng. Part H. J. Eng. Med.* 232, 323–343. doi:10.1177/0954411918759801

Kadry, G. (2019). Comparison between gelatin/carboxymethyl cellulose and gelatin/carboxymethyl nanocellulose in tramadol drug loaded capsule. *Heliyon* 5, e02404. doi:10.1016/j.heliyon.2019.e02404

Karimzadeh, S., and Farahpour, M. R. (2017). Topical application of Salvia officinalis hydroethanolic leaf extract improves wound healing process. *Indian J. Exp. Biol.* 55, 98–106.

Karoyo, A. H., and Wilson, L. D. (2021). A review on the design and hydration properties of natural polymer-based hydrogels. *Mater. (Basel)* 14, 1095. doi:10.3390/ma14051095

Koperska, M., Łojewski, T., and Łojewska, J. (2011). Vibrational spectroscopy to study degradation of natural dyes. Assessment of oxygen-free cassette for safe exposition of artefacts. *Anal. Bioanal. Chem.* 399, 3271–3283. doi:10.1007/s00216-010-4460-7

Li, Q., Wang, Z., Shi, N., Qi, Y., Yao, W., Yu, J., et al. (2023). Application and prospect of the therapeutic strategy of inhibiting cellular senescence combined with pro-regenerative biomaterials in regenerative medicine. *Smart Med.* 2. doi:10.1002/SMMD.20230030

Liu, J., Jiang, W., Xu, Q., and Zheng, Y. (2022). Progress in antibacterial hydrogel dressing. *Gels* 8, 503. doi:10.3390/gels8080503

Luo, Z., Wang, Y., Xu, Y., Wang, J., and Yu, Y. (2023). Modification and crosslinking strategies for hyaluronic acid-based hydrogel biomaterials. *Smart Med.* 2. doi:10.1002/SMMD.20230029

Marques, M. P., Mendonça, L., Neves, B. G., Varela, C., Oliveira, P., and Cabral, C. (2023). Exploring iberian peninsula lamiaceae as potential therapeutic approaches in wound healing. *Pharmaceuticals* 16, 347. doi:10.3390/ph16030347

Mattera, E., Iovene, M. R., Rispoli, C., Falco, G., Rocco, N., and Accurso, A. (2014). Assessment of bacterial infection in chronic wounds in the elderly: biopsy versus VERSAJET. *Int. J. Surg.* 12, S50–S55. doi:10.1016/j.ijsu.2014.08.381

Mircioiu, C., Voicu, V., Anuta, V., Tudose, A., Celia, C., Paolino, D., et al. (2019). Mathematical modeling of release kinetics from supramolecular drug delivery systems. *Pharmaceutics* 11, 140. doi:10.3390/pharmaceutics11030140

Mohamed, T. M., Attia, M. S., El-Sayyad, G. S., Fathy, R. M., and El-Batal, A. I. (2022). Gamma radiation crosslinking of PVA/myrrh resin thin film for improving the post-harvest time of lemon fruits. *RSC Adv.* 12, 5619–5628. doi:10.1039/d1ra09360f

Mot, M.-D., Gavrilaş, S., Lupitu, A. I., Moisa, C., Chambre, D., Tit, D. M., et al. (2022). Salvia officinalis L. Essential oil: characterization, antioxidant properties, and the effects of aromatherapy in adult patients. *Antioxidants* 11, 808. doi:10.3390/antiox11050808

Namjoyan, F., Kiashi, F., Moosavi, Z. B., Saffari, F., and Makhmalzadeh, B. S. (2016). Efficacy of Dragon's blood cream on wound healing: a randomized, double-blind, placebo-controlled clinical trial. *J. Tradit. Complement. Med.* 6, 37–40. doi:10.1016/j.jtcme.2014.11.029

Neres Santos, A., Duarte Moreira, A., Piler Carvalho, C., Luchese, R., Ribeiro, E., McGuinness, G., et al. (2019). Physically cross-linked gels of PVA with natural polymers as matrices for manuka honey release in wound-care applications. *Mater. (Basel)* 12, 559. doi:10.3390/ma12040559

Oliveira, A. S., Seidi, O., Ribeiro, N., Colaço, R., and Serro, A. P. (2019). Tribomechanical comparison between PVA hydrogels obtained using different processing conditions and human cartilage. *Mater. (Basel)* 12, 3413. doi:10.3390/ma12203413

Oliveira, R. N., Mancini, M. C., Oliveira, F. C. S. de, Passos, T. M., Quilty, B., Thiré, R. M. da S. M., et al. (2016). FTIR analysis and quantification of phenols and flavonoids of five commercially available plants extracts used in wound healing. *Matéria. Rio. Jan.* 21, 767–779. doi:10.1590/S1517-707620160003.0072

Ozcan, N., and Saloglu, D. (2015). Swelling kinetics and diffusion coefficients of polyacrylamide hydrogels via different drying methods. *J. Chem. Eng. Res. Updat.* 2, 51–56. doi:10.15377/2409-983X.2015.02.02.2

Pangesti, D. P., and Masruri, M. (2020). Consistency of spectra and antibacterial activity of the extract mixture of curcuma longa, zingiber officinale, and syzigium aromaticum. *IOP Conf. Ser. Mater. Sci. Eng.* 833, 012033. doi:10.1088/1757-899X/833/1/012033

Peng, J., Ellingham, T., Sabo, R., Clemons, C. M., and Turng, L.-S. (2015). Oriented polyvinyl alcohol films using short cellulose nanofibrils as a reinforcement. *J. Appl. Polym. Sci.* 132. doi:10.1002/app.42283

Peres, I. S. A., Conceição, K. A. O., Silva, L. A. F., Khouri, N. G., Yoshida, C. M. P., Concha, V. O. C., et al. (2023). Dragon's Blood: antioxidant properties for nutraceuticals and pharmaceuticals. *Rend. Lincei. Sci. Fis. Nat.* 34, 131–142. doi:10.1007/s12210-022-01122-4

Pettignano, A., Daunay, A., Moreau, C., Cathala, B., Charlot, A., and Fleury, E. (2019). Sustainable modification of carboxymethyl cellulose by passerini three-component reaction and subsequent adsorption onto cellulosic substrates. *ACS Sustain. Chem. Eng.* 7, 14685–14696. doi:10.1021/acssuschemeng.9b02634

Pieters, L., De Bruyne, T., Van Poel, B., Vingerhoets, R., Totté, J., Vanden Berghe, D., et al. (1995). *In vivo* wound healing activity of Dragon's Blood (Croton spp.), a traditional South American drug, and its constituents. *Phytomedicine Stuttg.* 2, 17–22. doi:10.1016/s0944-7113(11)80043-7

Ponco, A., and Helmiyati, H. (2020). Hydrogel of carboxymethyl cellulose and polyvinyl alcohol modified by CuNPs as antibacterial in wound dressing. doi:10.1063/5.0008096

Rajawasam, C. W. H., Dodo, O. J., Weerasinghe, M. A. S. N., Raji, I. O., Wanasinghe, S. V., Konkolewicz, D., et al. (2024). Educational series: characterizing crosslinked polymer networks. *Polym. Chem.* 15, 219–247. doi:10.1039/D3PY00914A

Reis, E. F. dos, Campos, F. S., Lage, A. P., Leite, R. C., Heneine, L. G., Vasconcelos, W. L., et al. (2006). Synthesis and characterization of poly (vinyl alcohol) hydrogels and hybrids for rMPB70 protein adsorption. *Mater. Res.* 9, 185–191. doi:10.1590/S1516-14392006000200014

Rempel, C., Zagonel, F. D., Silva, D. S. da, Marmitt, D. J., and Sehnem, E. (2020). Effect of the cream based on Croton lechleri Müll. Arg. in the treatment of diabetic patients' ulcers: a case study. *Cad. UniFOA* 15. doi:10.47385/cadunifoa.v15i44.3283

Restrepo, I., Medina, C., Meruane, V., Akbari-Fakhrabadi, A., Flores, P., and Rodríguez-Llamazares, S. (2018). The effect of molecular weight and hydrolysis degree of poly(vinyl alcohol)(PVA) on the thermal and mechanical properties of poly(lactic acid)/PVA blends. *Polímeros* 28, 169–177. doi:10.1590/0104-1428.03117

Ritger, P. L., and Peppas, N. A. (1987). A simple equation for description of solute release I. Fickian and non-fickian release from non-swellable devices in the form of slabs, spheres, cylinders or discs. *J. Control. Release* 5, 23–36. doi:10.1016/0168-3659(87)90034-4

Saidi, M., Dabbaghi, A., and Rahmani, S. (2020). Swelling and drug delivery kinetics of click-synthesized hydrogels based on various combinations of PEG and star-shaped PCL: influence of network parameters on swelling and release behavior. *Polym. Bull.* 77, 3989–4010. doi:10.1007/s00289-019-02948-z

Salazar, J. D. R. (2018). Study of structural, thermic, μ-Raman and optic transformation of PVA/TiO2 polymeric membranes. *Sci. Tech. Año XXIII, Univ. Tecnológica Pereira* 23, 543–552. doi:10.22517/23447214.15771

Salević, A., Stojanović, D., Lević, S., Pantić, M., Đorđević, V., Pešić, R., et al. (2022). The structuring of sage (Salvia officinalis L.) extract-incorporating edible zein-based materials with antioxidant and antibacterial functionality by solvent casting versus electrospinning. *Foods* 11, 390. doi:10.3390/foods11030390

Salguero, M., and Pilaquinga, F. (2017). Síntesis y caracterización de nanopartículas de plata preparadas con extracto acuoso de cilantro (Coriandrum sativum) y recubiertas con látex de Sangre de Drago (Croton lechleri). *infoANALÍTICA* 5, 9–23.

Setapa, A., Ahmad, N., Mohd Mahali, S., and Mohd Amin, M. C. I. (2020). Mathematical model for estimating parameters of swelling drug delivery devices in a two-phase release. *Polym. (Basel)* 12, 2921. doi:10.3390/polym12122921

Shabbir, M., Sajid, A., Hamid, I., Sharif, A., Akhtar, M. F., Raza, M., et al. (2018). Influence of different formulation variables on the performance of transdermal drug delivery system containing tizanidine hydrochloride: *in vitro* and *ex vivo* evaluations. *Braz. J. Pharm. Sci.* 54. doi:10.1590/s2175-97902018000400130

Sharratt, W. N., Lopez, C. G., Sarkis, M., Tyagi, G., O'Connell, R., Rogers, S. E., et al. (2021). Ionotropic gelation fronts in sodium carboxymethyl cellulose for hydrogel particle formation. *Gels* 7, 44. doi:10.3390/gels7020044

Siddaiah, T., Ojha, P., Kumar, N. O. G. V. R., and Ramu, C. (2018). Structural, optical and thermal characterizations of PVA/MAA:EA polyblend films. *Mater. Res.* 21. doi:10.1590/1980-5373-mr-2017-0987

Silva, P. H. da C., and Rodriguez, A. F. R. (2019). Síntese e caracterização de nanopartículas de ouro coloidal com o látex como um agente redutor. *Nativa* 7, 268. doi:10.31413/nativa.v7i3.6544

Siqueira, E. J., Brochier Salon, M.-C., and Mauret, E. (2015). The effects of sodium chloride (NaCl) and residues of cellulosic fibres derived from sodium carboxymethylcellulose (NaCMC) synthesis on thermal and mechanical properties of CMC films. *Ind. Crops Prod.* 72, 87–96. doi:10.1016/j.indcrop.2015.01.017

Soares, S., Peixoto, H., Prudencio, E., Luchese, R., Araújo, R., Moreira, A., et al. (2022). Biodegradable sodium carboxymethyl cellulose membranes containing melaleuca essential oils for wound care material. *Quim. Nova.* doi:10.21577/0100-4042.20170903

Somayeh Samaei, S., Khanmohammadi Khorrami, M., and Bagheri Garmarudi, A. (2021). Investigation the application of niosome as a nanocarrier for sage (Salvia officinalis L.) extract by spectroscopy and chemometrics. *Rev. del Cuerpo Médico Hosp. Nac. Almanzor Aguinaga Asenjo* 14, 155–162. doi:10.35434/rcmhnaaa.2021.142.1044

Takahashi, P. Y., Kiemele, L. J., and Jones, J. P. (2004). Wound care for elderly patients: advances and clinical applications for practicing physicians. *Mayo Clin. Proc.* 79, 260–267. doi:10.4065/79.2.260

Tarawneh, O., Hamadneh, I., Huwaitat, R., Al-Assi, A. R., and El Madani, A. (2021). Characterization of chlorhexidine-impregnated cellulose-based hydrogel films intended for the treatment of periodontitis. *Biomed. Res. Int.* 2021, 1–7. doi:10.1155/2021/9853977

Vigata, M., Meinert, C., Hutmacher, D. W., and Bock, N. (2020). Hydrogels as drug delivery systems: a review of current characterization and evaluation techniques. *Pharmaceutics* 12, 1188. doi:10.3390/pharmaceutics12121188

Wang, S., Shi, Y., Ma, J., Ye, Z., Yao, M., Shang, J., et al. (2023). Enhanced intradermal delivery of Dragon's blood in biocompatible nanosuspensions hydrogel patch for skin photoprotective effect. *J. Cosmet. Dermatol.* 22, 1046–1062. doi:10.1111/jocd.15515

Xiao, Y., Zhao, H., Ma, X., Gu, Z., Wu, X., Zhao, L., et al. (2022). Hydrogel dressing containing basic fibroblast growth factor accelerating chronic wound healing in aged mouse model. *Molecules* 27, 6361. doi:10.3390/molecules27196361

Xu, L., Zhou, Z., Chen, Y., Lu, H., and Hu, P. (2022). Resina draconis particles encapsulated in a hyaluronic-acid-based hydrogel to treat complex burn wounds. *Pharmaceutics* 14, 2087. doi:10.3390/pharmaceutics14102087

Yang, X., Wu, Y., Wei, K., Fang, W., and Sun, H. (2018). Non-isothermal crystallization kinetics of short glass fiber reinforced poly (ether ether ketone) composites. *Mater. (Basel)* 11, 2094. doi:10.3390/ma11112094

Yang, Y., Zhang, J., Liu, Z., Lin, Q., Liu, X., Bao, C., et al. (2016). Tissue-integratable and biocompatible photogelation by the imine crosslinking reaction. *Adv. Mater.* 28, 2724–2730. doi:10.1002/adma.201505336

Yu, J., Zhang, R., Chen, B., Liu, X., Jia, Q., Wang, X., et al. (2022). Injectable reactive oxygen species-responsive hydrogel dressing with sustained nitric oxide release for bacterial ablation and wound healing. *Adv. Funct. Mater.* 32. doi:10.1002/adfm.202202857

Zeinalipour-Yazdi, C. D., and Christofides, C. (2009). Linear correlation between binding energy and Young's modulus in graphene nanoribbons. *J. Appl. Phys.* 106, 054318. doi:10.1063/1.3211944

Zeleníková, R., and Vyhlídalová, D. (2019). Applying honey dressings to non-healing wounds in elderly persons receiving home care. *J. Tissue Viability* 28, 139–143. doi:10.1016/j.jtv.2019.04.002

Zhan, Y., and Chu, C.-C. (2002). Biodegradation of hydrophilic-hydrophobic hydrogels and its effect on albumin release. *J. Mater. Sci. Mater. Med.* 13, 667–676. doi:10.1023/a:1015785625547

Zhang, Y., Remadevi, R., Hinestroza, J. P., Wang, X., and Naebe, M. (2020). Transparent ultraviolet (UV)-Shielding films made from waste hemp hurd and polyvinyl alcohol (PVA). *Polym. (Basel)* 12, 1190–1214. doi:10.3390/polym12051190

Zhu, J., Li, Q., Che, Y., Liu, X., Dong, C., Chen, X., et al. (2020). Effect of Na2CO3 on the microstructure and macroscopic properties and mechanism analysis of PVA/CMC composite film. *Polym. (Basel)* 12, 453. doi:10.3390/polym12020453